Current Optics and Photonics
Vol. 1, No. 2, April 2017, pp. 132-137

ISSN: 2508-7266(Print) / ISSN: 2508-7274(Online)
DOI: https://doi.org/10.3807/COPP.2017.1.2.132

Demonstration of the Usefulness of Optical Coherence Tomography in Imaging a Mouse Tail Model of Lymphedema

Hui Dong Kim[1†], Dong Kyu Kim[1†], Yu-Gyeong Chae[2], Seok Gyo Park[1], Ghi Chan Kim[1], Ho Joong Jeong[1], Young-Joo Sim[1*], and Yeh-Chan Ahn[2]**

[1]*Department of Physical Medicine and Rehabilitation, College of Medicine, Kosin University, Busan 49267, Korea*
[2]*Department of Biomedical Engineering and Center for Marine-Integrated Biomedical Technology, Pukyong National University, Busan 48513, Korea*

(Received September 7, 2016 : revised December 2, 2016 : accepted January 5, 2017)

To investigate the usefulness of optical coherence tomography (OCT) for imaging lymphedema, we directly compared it to other histological methods in a mouse model of lymphedema. We performed detailed imaging of the lymphedema lesion on a mouse tail. We imaged the mouse tail *in vivo* with OCT and created histopathological samples. We constructed a spectrometer-based OCT system using a fiber-optic Michelson interferometer. The light was directed to 50:50 couplers that split the light into reference and sample arms. Backscattered light from a reference mirror and the sample produced an interference fringe. An OCT image of the lymphedema model revealed an inflammatory reaction of the skin that was accompanied by edema, leading to an increase in the light attenuation in the dermal and subcutaneous layers. Similar to OCT image findings, histological biopsy showed an inflammatory response that involved edema, increased neutrophils in epidermis and subdermis, and lymphatic microvascular dilatation. Furthermore, the lymphedema model showed an increase in thickness of the dermis in both diagnostic studies. In the mouse tail model of lymphedema, OCT imaging showed very similar results to other histological examinations. OCT provides a quick and useful diagnostic imaging technique for lymphedema and is a valuable addition or complement to other noninvasive imaging tools.

Keywords : Lymphedema, Optical coherence tomography, Mouse model, Animal experiment
OCIS codes : (170.6935) Tissue characterization; (170.3880) Medical and biological imaging; (170.4500) Optical coherence tomography

I. INTRODUCTION

Lymphedema causes local fluid retention and edema in subcutaneous tissue as a result of dysfunction in the circulating interstitial fluid between the thoracic duct and bloodstream due to damage or flaws in lymphatic systems [1, 2]. Penetration of inflammatory cells in lymphedema tissues damages dermal connective tissue elements, ground substances, microfilaments, collagen, and elastic fibers. As a result, angiogenic factors are generated by vascular endothelial and dermal inflammatory cells to cause vascular proliferation and angiosarcomas, leading to edema, chronic inflammation, fibrosis of tissue, and other conditions [3-6].

Tabibiazar et al. induced lymphedema in an animal model using a mouse tail, and observed an increase in fibroblast cells, hyperkeratosis, edema in epidermis, and expanded lymphatics in the dermis and subdermis in mouse tail histological samples [7].

Many progressive lymphedema patients can be diagnosed through distinguishing medical history, clinical features, and different imaging studies. Current diagnosis of lymphedema is done through the volume changes of affected limbs [8],

†The authors contributed equally to this work.
*Corresponding author: *oggum@hanmail.net, **ahny@pknu.ac.kr
Color versions of one or more of the figures in this paper are available online.

and the tests that can diagnose lymphedema include isotopic lymphoscintigraphy, indirect and direct lymphography, lymphatic capillaroscopy, magnetic resonance imaging (MRI), axial tomography and ultrasonography [9]. However early diagnosis may be difficult because these volume and tissue changes are not clearly observed in early stages of the disease. Various studies have attempted to diagnose lymphedema through the volume changes, but the definition of volume change varies among studies [10-14]. In addition, diagnosis is not easy in early stages of mild or intermittent edema [9, 15]. Diagnosis of early stage lymphedema requires an invasive histologic assessment. However, this may cause complications such as infection or worsening of edema, so it is limited in clinical application.

Optical coherence tomography (OCT) is a new optical diagnostic technology which was first introduced as an imaging assessment method of the retina by Huang et al. in 1991 [16]. This technology scans and radiates near-infrared light to the body, then measures the reflected light intensity in each tissue in different positions and obtains images of the tissue through computer signal processing. It is similar to ultrasonography, but uses light instead of sound to obtain near-histological resolution.

In the 1990s when OCT was first introduced, it was shown to be effective in obtaining a non-invasive, contactless high resolution image used to study structural changes in the retina and optic nerve head [17]. Studies using OCT allow the visualization of changes in muscle microstructure in Duchenne muscular dystrophy [18, 19] and observation of microarchitecture by comparing the OCT images of axillary lymph node and histologic findings of breast cancer patients [20, 21].

However, studies on OCT imaging of tissues in cases of lymphedema have not been reported. Therefore, we constructed a mouse tail model of lymphedema and compared the OCT image to histologic findings to determine the utility of OCT in imaging of lymphedema.

II. EXPERIMENTAL DETAILS

2.1. Animals and Ethical Approval

Two male mice from the Institute of Cancer Research were used in this study. The mouse body weights were approximately 170~220 g. The mice were acclimated for one week before the experiments. The room temperature was maintained at 22~23°C with a humidity of 50~55% and lighting was on a 12-hour light-dark cycle. A diet of commercial rodent pellets and water was supplied ad libitum. We conducted surgery to yield a lymphedema on mouse tails. All animal procedures were conducted in accordance with the guidelines published in the Guide for the Care and Use of Laboratory Animals (DHEW publication NIH 85-23, revised 2010, Office of Science and Health Reports, DRR/NIH, Bethesda, MD). The study protocol was approved by the Committee on Animal Research of the College of Medicine at Kosin University.

2.2. Surgery Procedures

Six-week-old mice were obtained to create a model of acute lymphedema. An additional group of unmanipulated normal mice was used for comparison. Before the surgery, the mice were anesthetized with Zoletil (0.04 ml/100 g body weight, intraperitoneal inj.) (Virbac, Carros, France) and Xylazine (0.01 ml/100 g body weight, intraperitoneal inj.) (Rompun, Bayer, Germany). To create a mouse tail model of acute secondary lymphedema, skin and subcutaneous tissues 5-10 mm from the tail base were removed without injury to the blood vessels on either side of the tail.

2.3. Optical Coherence Tomography System and Histopathology

OCT provides cross-sectional images of micro-tissue morphology with a high resolution (2-10 μm) in a non-invasive manner. OCT acquires images of tissue by illuminating a biological sample with a focused beam of near-infrared light, then detecting the light that is backscattered. Backscattering from different depths within the tissue is separated through a process referred to as interferometry which can achieve a narrow, one-dimensional depth scan into the tissue at a specific location. Different tissues have different scattering and absorption properties, allowing OCT to provide high-resolution morphologic imaging.

OCT was applied to image the detailed structure of the lymphedema lesion in the mouse tail in the second week. After *in vivo* OCT imaging was done, the mouse tail was cut off (5-10 mm from tail base) and immediately fixed in formalin solution. Paraffin blocks were made using the fixed mouse tail samples. The paraffin-embedded mouse tail samples were stained with hematoxylin-eosin to examine histological changes. Images of the stained slides were captured by a digital camera (Digital sight DS-U1, Nikon, Tokyo, Japan) attached to a microscope (Eclipse 80i, Nikon, Tokyo, Japan).

We constructed a spectrometer-based OCT system using a fiber-optic Michelson interferometer, as shown in Fig. 1. A broadband light was delivered to a fiber based 2×2 beam splitter through optical fiber and the split beams were directed to reference and sample arm. The beams were reflected by a reference mirror and sample surfaces in tissue under a two-axis scanner, respectively. Two beams, then, were interfered at the beam splitter and directed to the detection arm. We used a broadband light source (SLED Butterfly, EXALOS, Schlieren, Switzerland) with a center

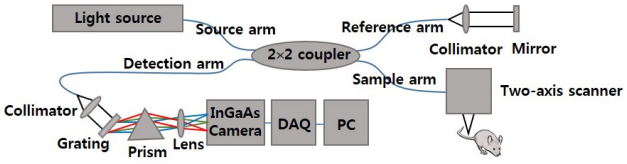

FIG. 1. Schematic diagram of homemade optical coherence tomography system.

wavelength of 1310 nm and a full width at half maximum of 80 nm. The two-axis scanner was customized using two galvanometers (6220H, Cambridge Technology, MA, USA) and had a maximum scanning area of 10.24×10.24 mm^2. The detection arm was composed of a grating (1145 lines/mm, Wasatch Photonics, NC, USA), a prism, and a line scan InGaAs camera with 1024 pixels and a line rate of 92 kHz (SU1024-LDH2, Goodrich, Princeton NJ, USA). We acquired volume images of each mouse tail with 1024×512×2048 voxels which corresponded to 5.12×2.3×10.24 mm^3. To obtain specifications of the OCT system, we measured the point spread function. The OCT system had a depth resolution of 11.629 μm in air (measured at a depth of 130 μm), an entire imaging depth of 2.3 mm, a roll-off distance of 1 mm at 5.65 dB power drop, a dynamic range of 106 dB, and a frame rate of 70 fps with 1024 A-lines.

III. RESULTS

Based on observation with the naked eye, the volume of the mouse tail gradually increased in lymphedema samples, reaching a maximum on the 14th day after the operation, and displaying twice as much volume as prior to the operation (Fig. 2).

In the OCT image of the epithelial layer of the mouse tail, the highest and second highest signal peaks provided information on the thickness of the epidermis, and the second and third highest signal peaks provided information on the thickness of the dermis. In the normal tail, an even surface and regular epidermal layer thickness were observed, and the distinctions between epidermis and dermis, and dermis and subcutaneous layer were relatively clear. However, in the lymphedema model, an uneven surface and irregular epidermal layer thickness were observed, and the boundaries between epidermis and dermis, and dermis and subcutaneous layer became unclear (Fig. 3).

Also, skin inflammation in the lymphedema model accompanied edema and displayed an increased light attenuation in the dermis and subcutaneous tissue (Fig. 3). Similar to OCT image findings, histological biopsy also showed an inflammatory response involving edema, more neutrophils in the epidermis and subdermis, and lymphatic microvascular

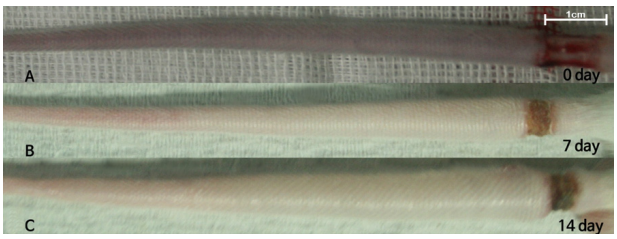

FIG. 2. These photos show changes in the edematous mouse tail over a 2-week period. Immediately after the operation (A), 7th day after the operation (B) and 14th day after the operation (C).

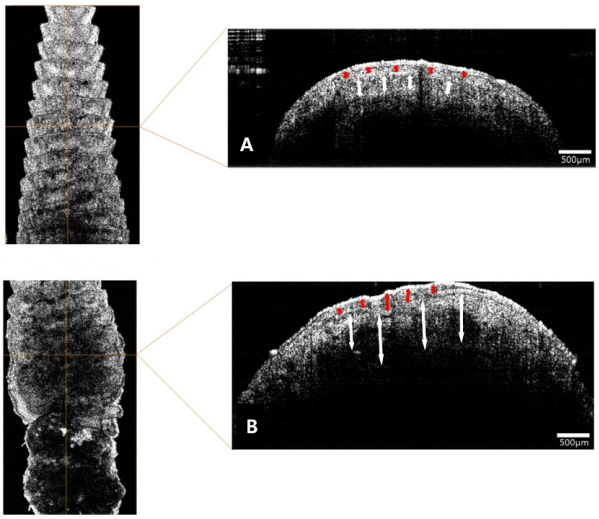

FIG. 3. *In vivo* 3D OCT images of mouse tail for normal (A) and lymphedema model (B). Left column shows *en face* images with 1024×2048 pixels (5.12×10.24 mm^2) and right column shows B-scan images with 1024×512 pixels (5.12×2.3 mm^2). Red and white double-headed arrows indicate the epidermal and dermal layer, respectively. In contrast to normal tissue, an inflammatory reaction of the skin leads to an increase in the light attenuation in the dermal and subcutaneous layers and an increase in the thickness of the dermis in the lymphedema model (white double-headed arrow). In the normal tail, an even surface and regular epidermal layer thickness were observed, and the distinctions between epidermis and dermis, and dermis and subcutaneous layer were relatively clear. However, in the lymphedema model, an uneven surface and irregular epidermal layer thickness were observed, and the boundaries between epidermis and dermis, and dermis and subcutaneous layer became unclear.

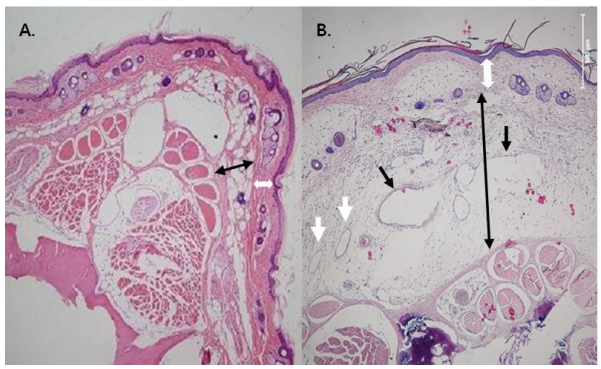

FIG. 4. Histopathology of mouse tail between normal (A) and lymphedema model (B). Normal tail skin harvested 18 mm from the base of the tail showed a thin epidermis and no dilated vessels in the dermis (A, H&E stain × 40). In contrast, the lymphedema model showed some dilated vessels (black arrows) and lymphatic microvascular cells (white arrow) with increasing thickness of the dermis (white double-headed arrow) and subcutaneous tissue (black double-headed arrow) (B, H&E stain x 40).

dilatation (Fig. 4). Furthermore, the lymphedema model showed an increase in thickness of the dermis using both methods.

IV. DISCUSSION

In this study, we created a mouse tail model of lymphedema to visualize using OCT, a real-time noninvasive high-resolution video imaging technology, and compared images to findings from histologic analysis. The usefulness of OCT as an imaging technology to diagnose and observe progress of lymphedema treatment was assessed through the results of this study.

The study of lymphedema requires an understanding through pathophysiologic analysis, but there are few experimental studies due to insufficient experimental subjects. As a result, treatment methods are applied to patients based on theoretical analyses. While there has been a long history of studying lymphedema, the mechanism behind its cause and histologic changes is still not clear, so it is often treated with a non-pharmacological method called complex decongestive physical therapy rather than medication. Therefore, development of a proper experimental model would greatly help the study and treatment of lymphedema.

Diagnosis of lymphedema can be made through the circumference difference in the limb, however this also varies in definition among studies [14, 22]. Additionally, the definition of lymphedema based on volume or circumference difference does not reflect changes in fluid, muscle mass, bone, fat or other tissue compositions [8].

Most patients with progressed lymphedema can be diagnosed based on specific clinical features and physical findings. However, in the early stage of lymphedema or for intermittent edema, it becomes difficult to make a differential diagnosis between lymphedema and other edematous states. In cases where a clear diagnosis of lymphedema cannot be made based solely on a physical examination, additional tests may be needed to determine if lymphatic function is damaged. Currently, isotopic lymphoscintigraphy is most commonly used and assesses the lymphatic function by visualizing major lymphatic trunks and lymph nodes. However, the histologic changes before and after lymphedema treatments cannot be observed through lymphatic function evaluation only, so an objective assessment of treatment effect cannot be made. Due to these limitations, lymphedema evaluation has recently been done using ultrasonography which allows the observation of cutaneous, epifascial and subfascial compartment thickening in lymphedema patients and can be used in differential diagnosis and therapeutic monitoring as well [1, 9].

Until now, many areas of medicine have attempted animal model tests using OCT imaging. In the 1990s when OCT was first introduced, it was shown to be effective in obtaining a non-invasive, contactless high resolution image used to study structural changes in the retina and optic nerve head [17]. The resolution of OCT imaging is approximately 2-10 μm, which is much higher than ultrasound (200 μm), MRI (1 mm) and computed tomography (300 μm). OCT also uses simple equipment and is less expensive than other imaging techniques. However, because of its low transmittance, it only transmits down to 1~2 mm from the surface of the body [23].

In other areas of study such as microvascular tissue and cancer, animal experimental models have recently been used to prove the clinical, diagnostic and therapeutic values of OCT [24, 25]. Also, McLaughlin et al. compared OCT imaging to histologic findings of axillary lymph nodes in breast cancer patients and found that OCT is useful for viewing microarchitecture and observing real-time node status in situ without the need for physical resection or histological processing during operation on breast cancer [20, 21].

Lymphedema typically accompanies inflammation, fibrosis, and adipose deposition, and the observation of chronic inflammation in the lymphedema area is critical for verifying treatment progress. Many cell types are involved in chronic inflammation, however macrophages are the main regulators of lymphangiogenesis and fibrosis [26]. Previous studies have visualized macrophages in coronary fibroatheroma using intravascular optical coherence tomography [27-30], so we used a mouse tail model of lymphedema and compared OCT imaging to histologic findings to examine the effectiveness of OCT in lymphedema diagnosis prior to clinically applying OCT for lymphedema verification.

In this study, OCT imaging showed that the mouse tail lymphedema model had a higher light attenuation in the dermal and subcutaneous layers compared to a normal mouse tail, presumably due to skin inflammation that accompanied the edema. Based on histological examination, more neutrophils and lymphatic microvascular dilatation were observed in the lymphedema model compared to normal tissue, which is also likely due to an inflammatory reaction from edema. In addition, increased dermis thickness was observed on the lymphedema model in both OCT and histological examination.

This study suggests that lymphedema can be effectively visualized with OCT in an animal model and OCT is a potential powerful tool that can be used to easily and non-invasively verify the increase in dermal thickness and inflammation changes in lymphedema when compared to histologic findings. In the future, high-resolution OCT imaging could be used to observe the sequence of histologic changes of lymphedema from the time of onset and non-invasively diagnose and verify treatment effects in humans. Using OCT to non-invasively verify the severity of inflammation of lymphedema territory would also be helpful in determining patients' treatment plans and measuring their progress.

This study was limited by the fact that it did not reach the statistical approach using OCT parameters when viewing the OCT image. However, this study provides a basic reference for studying the diagnosis of lymphedema using OCT.

V. CONCLUSION

In the mouse tail model of lymphedema, OCT imaging showed very similar results to corresponding histological examinations. OCT provides a quick and useful diagnostic imaging technique for lymphedema and is a valuable addition or complement to other noninvasive imaging tools.

ACKNOWLEDGMENT

This work was supported by Kosin Medical Development Foundation and National Research Foundation of Korea (2013S1A5A2A03045562).

REFERENCES

1. S. G. Rockson, "Lymphedema," Am. J. Med. **110**, 288-95 (2001).
2. A. Szuba and S. G. Rockson, "Lymphedema: anatomy, physiology and pathogenesis," Vasc. Med. **2**, 321-6 (1997).
3. J. Daróczy, "Pathology of lymphedema," Clin. Dermatol. **13**, 433-44 (1995).
4. A. G. Warren, H. Brorson, L. J. Borud, and S. A. Slavin, "Lymphedema: a comprehensive review," Ann. Plast. Surg. **59**, 464-72 (2007).
5. T. J. Ryan, "The lymphatics of the skin. in: the physiology and pathophysiology of the skin," London: Academic press **5**, 1755-80 (1978).
6. B. Battistini, P. D'Orléans-Juste, and P. Sirois, "Endothelins: circulating plasma levels and presence in other biologic fluids," Lab. Invest. **68**, 600-28 (1993).
7. R. Tabibiazar, L. Cheung, J. Han, J. Swanson, A. Beilhack, A. an, S. S. Dadras, N. Rockson, S. Joshi, R. Wagner, and S. G. Rockson, "Inflammatory manifestations of experimental lymphatic insufficiency," PLoS Med. **3**, 1114-1139 (2006).
8. K. C. Johnson, A. G. Kennedy, and S. M. Henry, "Clinical measurements of lymphedema," Lymphat. Res. Biol. **12**, 216-21 (2014).
9. A. Szuba and S. G. Rockson, "Lymphedema: classification, diagnosis and therapy," Vasc Med **3**, 145-156 (1998).
10. N. L. Stout, L. A. Pfalzer, E. Levy, C. McGarvey, B. Springer, L. H. Gerber, and P. Soballe, "Segmental limb volume change as a predictor of the onset of lymphedema in women with early breast cancer," PM R **3**, 1098-105 (2011).
11. S. A. Czerniec, L. C. Ward, K. M. Refshauge, J. Beith, M. J. Lee, S. York, and S. L. Kilbreath, "Assessment of breast cancer-related arm lymphedema--comparison of physical measurement methods and self-report," Cancer Invest **28**, 54-62 (2010).
12. A. W. Stanton, C. Badger, and J. Sitzia, "Non-invasive assessment of the lymphedematous limb," Lymphology **33**, 122-35 (2000).
13. J. M. Armer and B. R. Stewart, "A comparison of four diagnostic criteria for lymphedema in a post-breast cancer population," Lymphat. Res. Biol. **3**, 208-217 (2005).
14. S. Hayes, B. Cornish, and B. Newman, "Comparison of methods to diagnose lymphoedema among breast cancer survivors: 6-month follow-up," Breast Cancer Res. Treat. **89**, 221-6 (2005).
15. D. E. Gary, "Lymphedema diagnosis and management," J. Am. Acad. Nurse Pract. **19**, 72-78 (2007).
16. D. Huang, E. A. Swanson, C. P. Lin, J. S. Schuman, W. G. Stinson, W. Chang, M. R. Hee, T. Flotte, K. Gregory, C. A. Puliafito, and J. G Fujimoto, "Optical coherence tomography," Science **254**, 1178-81 (1991).
17. M. R. Hee, J. A. Izatt, E. A. Swanson, D. Huang, J. S. Schuman, C. P. Lin, C. A. Puliafito, and J. G Fujimoto, "Optical coherence tomography of the human retina," Archives of ophthalmology **113**, 325-32 (1995).
18. B. R. Klyen, J. J. Armstrong, S. G. Adie, H. G. Radley, M. D. Grounds, and D. D. Sampson, "Three-dimensional optical coherence tomography of whole-muscle autografts as a precursor to morphological assessment of muscular dystrophy in mice," J. Biomed. Opt. **13**, 11003 (2008).
19. B. R. Klyen, T. Shavlakadze, H. G. Radley-Crabb, M. D. Grounds, and D. D. Sampson, "Identification of muscle necrosis in the mdx mouse model of Duchenne muscular dystrophy using three-dimensional optical coherence tomography," J. Biomed. Opt. **16**, 076013 (2011).
20. F. T. Nguyen, A. M. Zysk, E. J. Chaney, S. G. Adie, J. G. Kotynek, U. J. Oliphant, F. J. Bellafiore, K. M Rowland, P. A. Johnson, and S. A. Boppart, "Optical coherence tomography: the intraoperative assessment of lymph nodes in breast cancer," IEEE Eng. Med. Biol. Mag. **29**, 63-70 (2010).
21. R. A. McLaughlin, L. Scolaro, P. Robbins, S. Hamza, C. Saunders, and D. D. Sampson, "Imaging of human lymph nodes using optical coherence tomography: potential for staging cancer," Cancer Res. **70**, 2579-2584 (2010).
22. S. A. McLaughlin, M. J. Wright, K. T. Morris, G. L. Giron, M. R. Sampson, J. P. Brockway, K. E. Hurley, E. R. Riedel, and K. J. Van zee, "Prevalence of lymphedema in women with breast cancer 5 years after sentinel lymph node biopsy or axillary dissection: objective measurements," J. Clin. Oncol. **26**, 5213-9 (2008).
23. W. Drexler, U. Morgner, R. K. Ghanta, F. X. Kärtner, J. S. Schuman, and J. G. Fujimoto, "Ultrahigh-resolution ophthalmic optical coherence tomography," Nat. Med. **7**, 502-7 (2001).
24. B. A. Standish, V. X. Yang, N. R. Munce, L. M. Wong Kee Song, G. Gardiner, A. Lin, Y. I. Mao, A. Vitkin, N. E. Marcon, and B. C. Wilson "Doppler optical coherence tomography monitoring of microvascular tissue response during photodynamic therapy in an animal model of Barrett's esophagus," Gastrointest. Endosc. **66**, 326-33 (2007).
25. T. Aoki, M. Rodriguez-Porcel, Y. Matsuo, A. Cassar, T. G. Kwon, F. Franchi, R. Gulati, S. S. Kushwaha, R. J. Lennon, L. O. Lerman, E. L. Ritman, and A. Lerman "Evaluation of coronary adventitial vasa vasorum using 3D optical coherence tomography--animal and human studies," Atherosclerosis **239**, 203-8 (2015).
26. S. Ghanta, D. A. Cuzzone, J. S. Torrisi, N. J. Albano, W. J. Joseph, I. L. Savetsky, J. C. Gardenier, D. Chang, J. Zampell, and B. J. Mehrara, "Regulation of inflammation and fibrosis by macrophages in lymphedema," Am. J. Physiol. Heart Circ. Physiol. **308**, 1065-77 (2015).
27. G. J. Tearney, H. Yabushita, S. L. Houser, H. T. Aretz, I. K. Jang, K. H. Schlendorf, C. R. Kauffman, M. Shishkov,

E. F. Halpern, and B. E. Bouma, "Quantification of macrophage content in atherosclerotic plaques by optical coherence tomography," Circulation **107**, 113-9 (2003).
28. M. Nakano, M. Vorpahl, F. Otsuka, M. Taniwaki, S. K. Yazdani, and A. V. Finn, "Ex vivo assessment of vascular response to coronary stents by optical frequency domain imaging," JACC Cardiovasc. Imaging **5**, 71-82 (2012).
29. M. Kashiwagi, L. Liu, K. K. Chu, C. H. Sun, A. Tanaka, J. A. Gardecki, and G. J. Tearney, "Feasibility of the assessment of cholesterol crystals in human macrophages using micro optical coherence tomography," PLoS One **9**, e102669 (2014).
30. L. Liu, J. A. Gardecki, S. K. Nadkarni, J. D. Toussaint, Y. Yagi, B. E. Bouma, and G. J. Tearney, "Imaging the subcellular structure of human coronary atherosclerosis using micro-optical coherence tomography," Nat. Med. **17**, 1010-4 (2011).